



HAL
open science

Probing the enpolarization phenomenon in a speckle pattern using a microwave photonics-inspired approach

Jonathan Staes, Julien Fade

► **To cite this version:**

Jonathan Staes, Julien Fade. Probing the enpolarization phenomenon in a speckle pattern using a microwave photonics-inspired approach. *Optics Letters*, 2024, 49 (15), pp.4330-4333. 10.1364/OL.530103 . hal-04699896

HAL Id: hal-04699896

<https://hal.science/hal-04699896v1>

Submitted on 14 Nov 2024

HAL is a multi-disciplinary open access archive for the deposit and dissemination of scientific research documents, whether they are published or not. The documents may come from teaching and research institutions in France or abroad, or from public or private research centers.

L'archive ouverte pluridisciplinaire **HAL**, est destinée au dépôt et à la diffusion de documents scientifiques de niveau recherche, publiés ou non, émanant des établissements d'enseignement et de recherche français ou étrangers, des laboratoires publics ou privés.

Probing the *enpolarization* phenomenon in a speckle pattern using a microwave photonics-inspired approach

JONATHAN STAES¹ AND JULIEN FADE^{1,2,*}

¹Univ Rennes, CNRS, Institut FOTON - UMR 6082, F-35000 Rennes, France

²Aix-Marseille Univ, CNRS, Centrale Med, Institut Fresnel, Marseille, France

*julien.fade@fresnel.fr

Compiled July 5, 2024

We report how Stokes polarimetry of a highly-resolved optical speckle pattern coupled to an original microwave photonics-inspired experimental approach allows a new light to be shedded on the so-called *enpolarization* phenomenon, which consists in the local increase of the light degree of polarization (DOP) inducing a high average DOP value after interaction of unpolarized light with a totally depolarizing sample.

<http://dx.doi.org/10.1364/ao.XX.XXXXXX>

Light depolarization mechanisms at the speckle grain scale, observable in coherent light, remain a current subject of interrogation, with experimental studies initially conducted over a statistical population of speckle grains [1–3], and more recently probing the state of polarization (SOP) of light in a deterministic manner across a highly-resolved speckle pattern [4–9]. Adopting the classical scheme of active polarimetric imaging, all these studies used a single-mode polarized illumination (laser), nevertheless similar analyses can be carried out under different illumination conditions. For example, the phenomenon known as “*enpolarization*” [10] was experimentally observed with a similar imaging setup under unpolarized coherent illumination [11, 12]. This apparently surprising phenomenon arises when a depolarized coherent beam interacts with a scattering depolarizing material and consists in the local increase of the degree of polarization (DOP) across the produced speckle pattern, which results in a high average DOP value after interaction of unpolarized light with a totally depolarizing sample [11–13]. In this Letter, we show how an original approach inspired from microwave photonics techniques allows one to probe and investigate this phenomenon, and provides a simple heuristic to understand the statistical properties of the DOP distribution [13].

The experiment reported here relies on an optimized Stokes polarimetry bench resolved at the speckle grain scale [4, 7–9]. This setup, which will not be detailed here for the sake of concision, uses a voltage-controlled polarization-state-analyzer (PSA) combining two liquid-crystal variable retarders and a fixed linear polarizer to probe the SOP of the light backscattered by the sample in a reflection configuration, at each location of the speckle pattern, allowing the SOP to be precisely measured locally across the highly resolved speckle pattern. Complete details about the setup can be found in [7], while the optimized

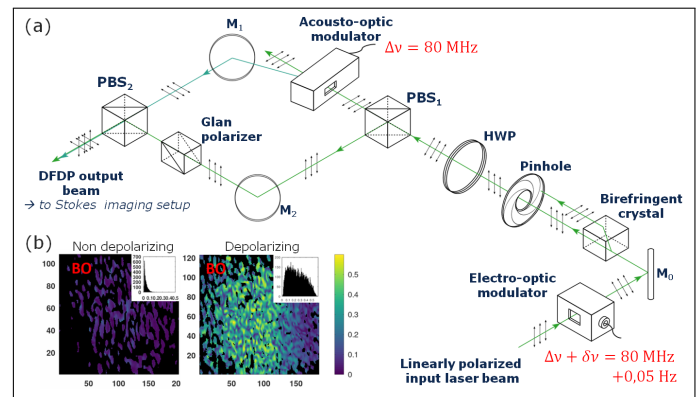


Fig. 1. (a) Sketch of the DFDP laser source with EO intensity modulation for frequency down-conversion of the RF beatnote. (b) OB contrast images acquired on a highly resolved speckle pattern produced by a non-depolarizing and a depolarizing sample under unpolarized illumination (after thresholding of the S_0 image above 10% of the maximum intensity).

estimation/processing protocol is detailed in [8]. For the present study, we engineered a versatile coherent illumination source by modifying the laser illumination using the setup of Fig. 1.a, and we complemented the previous Stokes imaging acquisitions with a so-called orthogonality-breaking (OB) polarimetry acquisition modality, a technique developed at Institut Foton since 2011 [14–17]. To this aim, the linearly polarized single-mode laser (COHERENT Verdi at $\lambda = 532$ nm) is fed into a polarization-sensitive Mach-Zehnder interferometer (MZI) architecture with acousto-optic-based frequency shift ($\Delta\nu = 80$ MHz) in one of the arms [15]. With such setup, we obtain a dual-frequency dual-polarization (DFDP) coherent source, whose average behavior when “seen” by a very low bandwidth camera is equivalent to a perfectly depolarized coherent illumination [18]. This module thus enables us to map the SOP of a speckle pattern resolved at the speckle grain scale under 3 different illuminations: (i) horizontal linear polarization, (ii) vertical, and (iii) depolarized illumination (sum of two balanced orthogonal, frequency-shifted polarizations). Indeed, switching between the three illumination modes is simply performed by appropriately rotating the half-wave plate (HWP) ahead of the MZI module.

Not only does this module make it possible to easily produce a fully coherent unpolarized illumination [18], but it also allows us to perform an additional imaging measurement based on the OB technique, which consists in measuring the radiofrequency (RF) beatnote (in amplitude and phase) produced at the offset frequency $\Delta\nu$ upon interaction of the DFDP beam with a sample [14]. The amplitude of this beatnote, referred to as OB contrast or OB rate, and denoted τ in the following, can indeed be linked to some polarimetric properties of the probed samples [14–17]. However, previous implementations relied on laser scanning imaging and direct demodulation on a fast photodetector, which is not possible with the (low bandwidth) CMOS camera involved in the experiment. We thus resorted to a frequency down-conversion approach (similar to the one used in [18]) to perform full-field OB imaging on the camera: as sketched in Fig. 1.a, an external electro-optical modulator (EOM) (custom 80 MHz resonant EOM, Thorlabs EO-AM-R-80-C4) with optical axes oriented at 45° from the input linear polarization, associated with a linear polarizer (operated with a Quartz beam-displacer, i.e., a birefringent crystal with optical axis at 45° from the propagation axis, and a pinhole to select the vertical output polarization), makes it possible to modulate the intensity of the input laser at a frequency $\Delta\nu + \delta\nu$, with a very low detuning frequency $\delta\nu \sim 0.05$ Hz, resulting in a shift of the relevant OB information to the difference frequency $\delta\nu \sim 0.05$ Hz. The low frequency beatnote is finally demodulated in amplitude and phase from the images stack using a standard 4-bucket demodulation scheme (i.e., acquiring typically with 1 s exposure time, and 0.2 Hz framerate), hence enabling full-field measurement of the OB contrast over the whole speckle pattern. Lastly, it must be noted that the OB acquisition is performed first, with the polarizer of the PSA removed from the Stokes imaging setup, since the purpose of OB is to probe the loss of polarization orthogonality induced by the sample itself and not by an external optical device such as the analyzer. Then, the 3 Stokes acquisitions mentioned above are carried out according to the procedures detailed in [7, 8], after a careful speckle registration procedure, similar to the one proposed in [4], in order to ensure that reintroducing the polarizer in the PSA does not modify the speckle wavefront to be analyzed.

In this study, for the sake of easy interpretation of the experimental results, the acquisitions are performed on two samples of opposite polarimetric nature: the first one is a non-depolarizing flat metal plate, which almost does not alter the SOP of the input light; the second one being a highly scattering and highly depolarizing flat piece of Spectralon [7]. For each sample, 4 acquisitions are carried out, namely: OB imaging under DFDP illumination; Stokes imaging with unpolarized illumination using the DFDP source (denoted \updownarrow); Stokes imaging with vertical (\uparrow) and then horizontal (\rightarrow) input polarization.

Table 1. Intercorrelation between intensity (S_0) images.

[Reference image: \updownarrow]	\rightarrow	\uparrow	OB
Non-depolarizing sample	90%	92%	87%
Depolarizing sample	55%	49%	83%

Let us first analyze the results obtained at a “macroscopic” scale across the whole speckle field imaged, comprising about 500-1000 resolved speckle grains on the detector, as can be seen in [7] or in the OB maps displayed in Fig. 1.b. We first analyze the

statistical properties of the total intensity images (S_0 Stokes parameter) acquired on the two samples. In particular, we provide in Table 1 the intercorrelation between the four S_0 images measured. Since it is established that on a perfectly non-depolarizing sample the speckle pattern should remain unchanged whatever be the SOP of the illumination [4], such measures performed on the metal blade reported in the first row of the table allow us to confirm the validity and stability of the experimental setup. Indeed, almost perfect correlation between the 3 Stokes acquisitions is observed, along with a slight decrease of the intercorrelation value for the OB acquisition which, as stated above, requires a slight modification of the PSA optical setup. On the other hand, when the Spectralon sample is considered, the two images acquired under unpolarized DFDP illumination (OB acquisition and first Stokes acquisition \updownarrow) remain quite correlated between them (83%), whereas the intercorrelation drops down by a factor of two when fully polarized illumination is used (\rightarrow or \uparrow). Such property is one of the elements of understanding of the *depolarization* phenomenon, as will be discussed below.

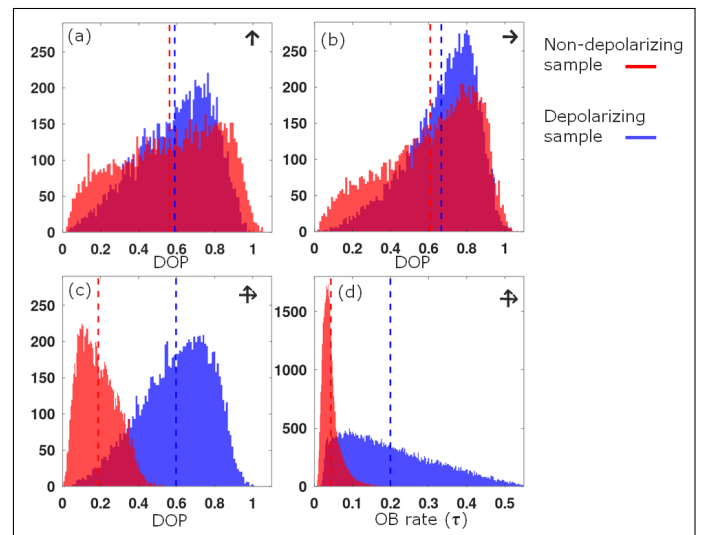


Fig. 2. Histograms of the local DOP under vertically (a), horizontally (b) polarized illumination. Histograms of DOP (c) and OB contrast (d) with unpolarized DFDP illumination (\updownarrow).

For the sake of concision, we do not report here the Stokes polarization images (S_1 , S_2 and S_3) acquired. However, the experimental results allowed us to check that, under polarized illumination, the incident SOP was well maintained on a non-depolarizing sample. On the other hand, for the Spectralon, it was checked that at each location of the speckle pattern the SOP was well defined (i.e., with DOP values close to 1), with values of S_1 , S_2 and S_3 spanning over the interval $[-1; 1]$ resulting in complete coverage of the Poincaré sphere. These results are in agreement with previous works [4, 7, 9], and are also confirmed by the shape of the estimated DOP histograms plotted in Fig. 2.a and 2.b, which show significantly high values of the DOP across the image for the two samples. The similarity between the distributions and average DOP values, despite the very different nature of the samples, can be explained by the fact that locally, at the speckle grain scale, the SOPs are perfectly defined when the illumination is single-mode (monochromatic, single polarization) [4, 7, 9].

In contrast to single-mode illumination, however, the histograms of the DOP under unpolarized DFDP illumination dis-

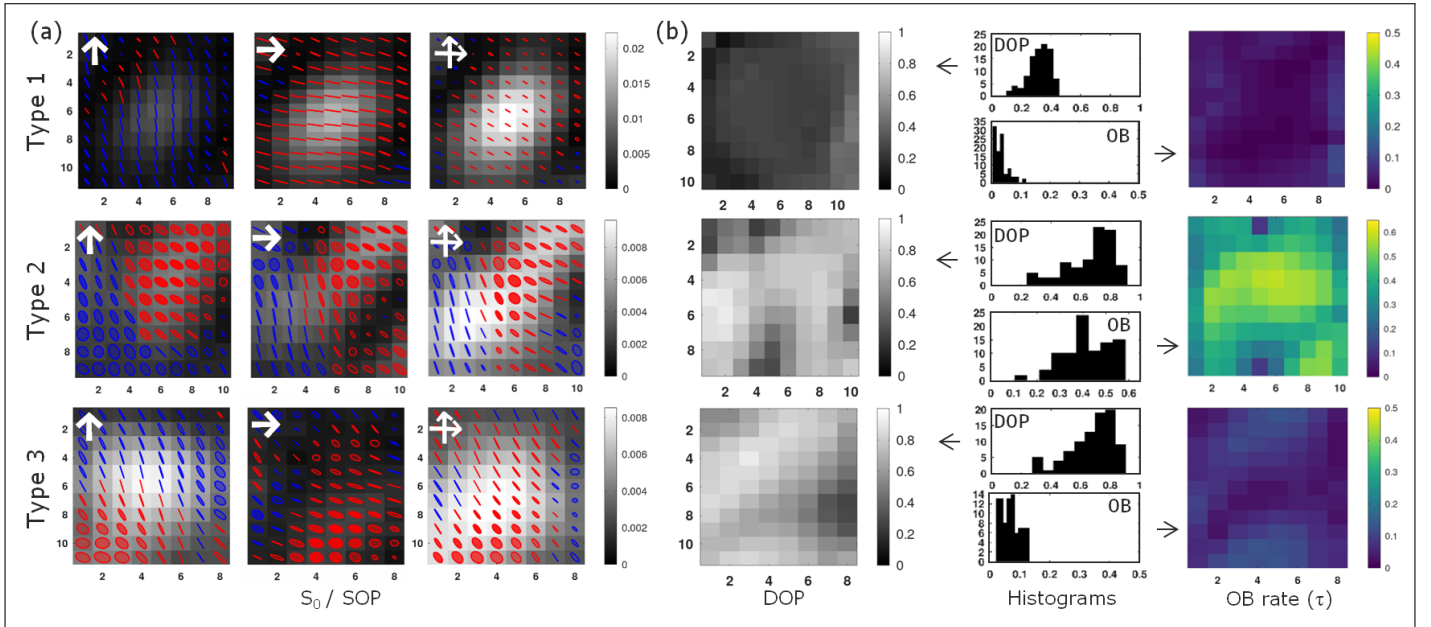


Fig. 3. (a) Intensity distribution (S_0 , in graylevels) and SOP representation (blue/red ellipses) of speckle grains of types 1, 2 and 3 under various illumination conditions (left: vertically polarized, center: horizontally polarized, right: unpolarized) on the Spectralon sample. (b) Local DOP (left) and amplitude of the detected OB beatnote (right), and corresponding histograms (center).

played in Fig. 2.c show two very distinct shapes for the two types of materials. The respective averages of these DOP distributions are 0.18 and 0.60, clearly revealing the opposite polarimetric nature of these samples. On the one hand, it is expected that the metallic blade should exhibit unpolarized speckle grains, since, as seen above, each component of the DFDP beam leads to similar patterns. The incoherent summation of these two speckle patterns with crossed linear polarizations hence produces an unpolarized speckle, with low average local DOP. On the other hand, the occurrence of high DOP values observed in Fig. 2.c for the Spectralon precisely correspond to the *enpolarization* phenomenon [11]. It can be noted however that the measured histogram does not strictly follow the theoretical parabolic-shaped probability density function of the DOP (i.e., $f_P(P) = 3P^2$ with P denoting the DOP [13]). The decrease of the histogram values at high DOP is due to the fact that the intensity images acquired have been thresholded so as to discard regions of the image with grayscale values below 10% of the maximum intensity. Another consequence of rejecting such regions showing poor level of confidence in the measured SOP [7] is the slight underestimation of the average DOP value in the reported experiments.

Interestingly, the difference in the polarimetric nature of the two samples is also clearly visible in the maps of the OB contrast measured. These maps and their corresponding histograms are displayed respectively in Fig. 1.b and Fig. 2.d, showing averages of 0.04 for the non-depolarizing sample and 0.19 for the depolarizing sample. This result could be expected since the orthogonality of the two polarization states of the DFDP source is more likely to be altered when such a beam interacts with a depolarizing sample, thus breaking the polarization orthogonality (hence inducing high τ values). This property is precisely the basis of the OB sensing approaches [14–17]. This result shows that full-field OB imaging, which can be operated with the proposed setup, can be an alternative approach to probe the *enpolarization* phenomenon and its properties without necessarily requiring the full-Stokes imaging architecture used in previous works.

Once analyzed the macroscopic properties of the DOP and OB contrast distributions across the whole speckle patterns, let us now focus at a more local scale on the behaviour of individual speckle grains obtained experimentally. Analyzing these particular cases will lead us to propose a fairly clear interpretation of the *enpolarization* phenomenon observed here macroscopically. According to the above discussion about intercorrelation of speckle intensity images acquired under distinct illumination polarizations, the speckle grains can be schematically categorized into “monomode” grains and “dual-mode” grains: in the first case, a bright grain obtained under vertically polarized (\uparrow) illumination, for instance, correspond to a dark intensity (“dark” grain) when the sample is enlightened with horizontal (\rightarrow) polarization. Contrarily, dual-mode bright grains exhibit high intensity (S_0) values under both polarizations. Following the above discussion, when illuminated with unpolarized (or DFDP) light, a perfectly non-depolarizing sample will produce only dual-mode grains, while a perfectly depolarizing one will schematically create about 50% of each category of grains.

The experimental results of Stokes and OB imaging of highly resolved speckle grains presented in Fig. 3 follow this basic categorization, with the first two rows addressing dual-mode grains, and the third one a monomode grain. The first special case identified (and referred to here as *Type 1* grain) occurs when the sample locally induces a unitary polarization transformation, thereby preserving the orthogonality between the two input polarization states. This is the only case observed on a non-depolarizing sample such as the metal plate studied (but whose results are not reported here for the sake of concision), leading to an unpolarized speckle grain under DFDP illumination with no OB beatnote creation. This situation is also likely to be encountered with a highly depolarizing sample such as the Spectralon, as exemplified in the first row of Fig. 3.a. A spatial average of the local DOP of 0.72 and 0.80 respectively is observed under cross-polarized illuminations, each of which being well preserved in the grain. It can also be seen (Fig. 3.b, left) and

corresponding histogram (Fig. 3.b, center) that the DOP under DFDP illumination is strongly diminished as it only reaches in average 0.30 across this grain (the non-zero DOP value being due to the intensity mismatch of the two grains observed under cross-polarized illuminations). Thanks to the setup proposed in this Letter, the preservation of polarimetric orthogonality is here confirmed from the estimated OB contrast map (Fig. 3.b, right) and the corresponding histogram (Fig. 3.b, center) which exhibit very low values of the OB contrast across the whole grain.

When the sample analyzed is not strictly non-depolarizing, the two incident polarization states (\uparrow and \rightarrow) are not likely to be preserved nor modified by the same Jones transformation in all dual-mode speckle grains. In such a situation, one expects a degradation of the polarization orthogonality and hence the occurrence of an OB “beatnote speckle” (as displayed in Fig. 1.b, right). This must be accompanied with an increase of the local DOP measured under unpolarized illumination (i.e. *enpolarization*) in such particular grains (the DOP value possibly reaching 1, if the intensities of the two modes are equal and if the resulting polarizations are identical). An example of such a typical extreme case, referred to here as *Type 2* grain, has been observed in the speckle pattern acquired on the depolarizing Spectralon sample and is provided in the second row of Fig. 3.

We present in the third row of Fig. 3 the last situation of a monomode grain, also observed on the depolarizing Spectralon sample. In this example of grains referred to here as *Type 3*, constructive interference produces a bright speckle grain under vertically polarized illumination, whereas in horizontally polarized illumination the interference is destructive. Therefore, the speckle grain obtained under unpolarized DFDP illumination is roughly similar in terms of intensity and of SOP to that obtained with vertical illumination, hence exhibiting a high value of the local DOP and contributing to the *enpolarization* effect. However, as can be seen in Fig. 3.c, this case does not produce any OB beatnote as the light detected in this type of grain is monomode.

Finally, the results presented in this Letter tend to show that the *enpolarization* phenomenon arises from two properties of speckle patterns which differ according to the polarimetric nature of the sample: (i) the spatial distribution of speckle grains for each of two orthogonally-polarized illumination modes, which are fully correlated for a non-depolarizing sample, but partially correlated for a fully depolarizing sample; and (ii) the ability of the material to alter the incident SOP (no alteration for a non-depolarizing sample, but possible alteration for a depolarizing sample). The above results now allow us to interpret quite clearly the theoretical average value of the DOP of $3/4$ expected in such experiment of *enpolarization* of a depolarized light by a depolarizing material [13]. Indeed, in this situation, the speckle patterns for each illumination mode show an intercorrelation as low as $\sim 50\%$, so we expect that around half of the grains observed under DFDP illumination correspond to single-mode grains, while the remaining half are dual-mode. For the former monomode grains, the DOP observed under DFDP illumination is maximal and the OB contrast is null. Now, for all the dual-mode grains, we expect a random distribution of SOPs, with a distribution of dual-mode grains ranging between the extreme cases of *Type 1* and *Type 2* grains discussed above, i.e., with DOP values between 0 and 1, and OB contrast ranging from 0 to 100%. Globally, spatial averaging over this population of dual-mode grains leads to an average DOP of 0.5 and a mean OB rate of 50% too. When we now extend this statistical reasoning to encompass the remaining population of single-mode grains (all sharing a unit DOP and zero OB contrast), we ob-

tain an expected average DOP over all grains of 0.75, and an expected OB rate of 25%. Such analysis is in reasonably fair agreement with the quantitative results obtained. Indeed, despite the consequences of experimental imperfections and of images thresholding discussed above, we obtained an average DOP of 0.60, and an average OB rate of 19%.

Using a specific DFDP laser source as a “controlled” model of unpolarized coherent source, we have shown that the *enpolarization* phenomenon could be experimentally probed with the full-field OB technique proposed, instead of using a full Stokes imaging approach which requires a more complex polarization-analyzing setup at the detection side. In addition, such source precisely corresponds to the physical model of unpolarized light used in [13], described as an incoherent sum of two cross-polarized coherent modes. It also reproduces the beam produced by an unpolarized He:Ne laser source such as the one used in [11], since in such laser, consecutive longitudinal modes exhibit cross-polarized SOPs. Following the method proposed in [18], this DFDP source would allow to extend these investigations to a more sophisticated model of unpolarized coherent source involving fast scanning of all SOPs across whole the Poincaré sphere, but also to the case of partially-polarized coherent illumination with controlled DOP. Deeper investigation of the correlation properties of speckles produced on a scattering sample with different polarizations of the illumination source also appears as an interesting perspective.

Acknowledgments. The authors thank Ph. Réfrégier and the DOP team of the Institut Foton for fruitful discussions.

Disclosures. The authors declare no conflicts of interest.

Data availability. Data underlying the results presented in this paper are not publicly available at this time but may be obtained from the authors upon reasonable request.

REFERENCES

1. P. Hariharan, *Opt. Acta: Int. J. Opt.* **24**, 979 (1977).
2. P. Elies, B. L. Jeune, F. L. Roy-Brehonnet, *et al.*, *J. Phys. D: Appl. Phys.* **30**, 29 (1997).
3. J. Broky and A. Dogariu, *Opt. Express* **18**, 20105 (2010).
4. L. Pouget, J. Fade, C. Hamel, and M. Alouini, *Appl. optics* **51**, 7345 (2012).
5. A. Ghabbach, M. Zerrad, G. Soriano, and C. Amra, *Opt. Express* **22**, 14594 (2014).
6. J. Dupont, X. Orlik, A. Ghabbach, *et al.*, *Opt. Express* **22**, 24133 (2014).
7. J. Staes and J. Fade, *JOSA A* **41**, 789 (2024).
8. J. Staes and J. Fade, *JOSA A* **41**, 800 (2024).
9. J. Staes and J. Fade, *JOSA A* **41**, 811 (2024).
10. R. Barakat, *Opt. Commun.* **123**, 443 (1996).
11. J. Sorrentini, M. Zerrad, G. Soriano, and C. Amra, *Opt. Express* **19**, 21313 (2011).
12. A. Ghabbach, M. Zerrad, G. Soriano, *et al.*, *Opt. express* **22**, 21427 (2014).
13. P. Réfrégier, M. Zerrad, and C. Amra, *Opt. Lett.* **37**, 2055 (2012).
14. J. Fade and M. Alouini, *Phys. Rev. Lett.* **109**, 43901 (2012).
15. E. Schaub, J. Fade, N. Ortega-Quijano, *et al.*, *J. Opt.* **16**, 122001 (2014).
16. N. Ortega-Quijano, J. Fade, M. Roche, *et al.*, *J. Opt. Soc. Am. A* **33**, 434 (2016).
17. R. Desapogu, G. Le Marchand, R. Smith, *et al.*, *Biomed. optics express* **12**, 5290 (2021).
18. N. Ortega-Quijano, J. Fade, F. Parnet, and M. Alouini, *Opt. Lett.* **42**, 2898 (2017).

REFERENCES

- 345
346 1. P. Hariharan, "Statistics of speckle patterns produced by a rough metal
347 surface," *Opt. Acta: Int. J. Opt.* **24**, 979–987 (1977).
- 348 2. P. Elies, B. L. Jeune, F. L. Roy-Brehonnet, *et al.*, "Experimental investi-
349 gation of the speckle polarization for a polished aluminium sample," *J.*
350 *Phys. D: Appl. Phys.* **30**, 29 (1997).
- 351 3. J. Broky and A. Dogariu, "Complex degree of mutual polarization in
352 randomly scattered fields," *Opt. Express* **18**, 20105–20113 (2010).
- 353 4. L. Pouget, J. Fade, C. Hamel, and M. Alouini, "Polarimetric imaging
354 beyond the speckle grain scale," *Appl. optics* **51**, 7345–7356 (2012).
- 355 5. A. Ghabbach, M. Zerrad, G. Soriano, and C. Amra, "Accurate metrology
356 of polarization curves measured at the speckle size of visible light
357 scattering," *Opt. Express* **22**, 14594–14609 (2014).
- 358 6. J. Dupont, X. Orlik, A. Ghabbach, *et al.*, "Polarization analysis of
359 speckle field below its transverse correlation width: application to
360 surface and bulk scattering," *Opt. Express* **22**, 24133–24141 (2014).
- 361 7. J. Staes and J. Fade, "Optimized stokes imaging for highly resolved
362 optical speckle fields, part i: optimized experimental setup," *JOSA A*
363 **41**, 789–799 (2024).
- 364 8. J. Staes and J. Fade, "Optimized stokes imaging for highly resolved op-
365 tical speckle fields, part ii: optimal acquisition and estimation strategies,"
366 *JOSA A* **41**, 800–810 (2024).
- 367 9. J. Staes and J. Fade, "Optimized stokes imaging for highly resolved
368 optical speckle fields, part iii: topological analysis of polarimetric state
369 distributions with optimized data representations," *JOSA A* **41**, 811–823
370 (2024).
- 371 10. R. Barakat, "Polarization entropy transfer and relative polarization
372 entropy," *Opt. Commun.* **123**, 443–448 (1996).
- 373 11. J. Sorrentini, M. Zerrad, G. Soriano, and C. Amra, "Enpolarization of
374 light by scattering media," *Opt. Express* **19**, 21313–21320 (2011).
- 375 12. A. Ghabbach, M. Zerrad, G. Soriano, *et al.*, "Depolarization and en-
376 depolarization dop histograms measured for surface and bulk speckle
377 patterns," *Opt. express* **22**, 21427–21440 (2014).
- 378 13. P. Réfrégier, M. Zerrad, and C. Amra, "Coherence and polarization
379 properties in speckle of totally depolarized light scattered by totally
380 depolarizing media," *Opt. Lett.* **37**, 2055–2057 (2012).
- 381 14. J. Fade and M. Alouini, "Depolarization remote sensing by orthogonality
382 breaking," *Phys. Rev. Lett.* **109**, 43901 (2012).
- 383 15. E. Schaub, J. Fade, N. Ortega-Quijano, *et al.*, "Polarimetric contrast
384 microscopy by orthogonality breaking," *J. Opt.* **16**, 122001 (2014).
- 385 16. N. Ortega-Quijano, J. Fade, M. Roche, *et al.*, "Orthogonality-breaking
386 sensing model based on the instantaneous Stokes vector and the
387 Mueller calculus," *J. Opt. Soc. Am. A* **33**, 434–446 (2016).
- 388 17. R. Desapogu, G. Le Marchand, R. Smith, *et al.*, "Label-free microscopy
389 of mitotic chromosomes using the polarization orthogonality breaking
390 technique," *Biomed. optics express* **12**, 5290–5304 (2021).
- 391 18. N. Ortega-Quijano, J. Fade, F. Parnet, and M. Alouini, "Generation of a
392 coherent light beam with precise and fast dynamic control of the state
393 and degree of polarization," *Opt. Lett.* **42**, 2898–2901 (2017).